INTERMEDIATE BANDS AND NON-RADIATIVE RECOMBINATION

César Tablero, Antonio Martí, David Fuertes Marrón, Elisa Antolín and Antonio Luque
Instituto de Energía Solar –Universidad Politécnica de Madrid
ETSI de Telecomunicación, Ciudad Universitaria, 28040 Madrid, Spain.
Email: ctablero@etsit.upm.es, Tfn: +34 91 5446341

ABSTRACT: The use of half-filled intermediate band materials has been proposed as a means to implement solar cells with efficiency exceeding that of single gap solar cells. An *intermediate band* can be regarded, at first, as a mere collection of energy levels within the semiconductor bandgap. However, its recombination properties are expected to be different from those traditionally attributed to deep levels. Hence, while deep centers behave mainly as non-radiative recombination centers, the IB is expected to exhibit negligible non-radiative recombination. It is the purpose of this work to study these phenomena by exploiting computational models based on ab-initio calculations.

Keywords: Intermediate Band, Impurities, Recombination, Solar Cell Efficiencies, Fundamentals, II-VI Semiconductors.

1 INTRODUCTION

Most point defects and impurities occur, when introduced in the lattice host, in multiple charge states that introduce transition energy levels that are located within the bandgap of the host semiconductor. Many properties of the host are consequently affected as, for example, those associated to charge-transfer processes between bands. The equilibrium positions of the atoms for different charge states of the impurity or defect are not necessarily the same. It is this difference what allows non-radiative recombination (NRR) via multi-phonon emission (MPE) after relaxation from one equilibrium position to another.

The MPE mechanism, [1] that takes place when an impurity is present, occurs basically in two capture steps. This can be illustrated with the help of a configuration coordinate diagram ((Figure 1) where Q represents a generalized relevant nuclear coordinate associated with the impurity/point defect and the curves represent the energy of the impurity/point system for the different states as functions of Q. For example, an electron in the conduction band (e_{CB}) is first captured into an impurity state ($D^{\alpha-1}+e_{CB} \rightarrow D^{\alpha}$) around the crossing point Q_C and then the electron recombines with a hole in the valence band (hole capture $D^{\alpha}+h_{VB} \rightarrow D^{\alpha-1}$ or $D^{\alpha} \rightarrow D^{\alpha-1}+e_{VB}$, where e_{VB} and h_{VB} represent a electron and a hole in the VB respectively) around crossing point Q_V . After the capture, there is a large modification of the impurity equilibrium position. The large vibrational energy, which is initially localized at the impurity center, will propagate away from the center in the form of lattice phonons. This mechanism of recombination gives rise to violent, short-lived, lattice vibrations localized at the defect which greatly enhance the probability of defect motion. For deep gap levels, in many cases, this lattice vibration is a breathing relaxation, as explained below, where the surrounding host atoms can undergo large displacements.

Each step of this mechanism is easy to model by considering the mean distortions of the configuration coordinates Q and of the restoring force constants associated with changes in the energy. In many cases Q is best thought of as corresponding to a breathing mode, that is, the symmetric inward or outward movement of the nearest neighbors. The state-dependence of the force which drives the distortion mainly comes from the state-dependent charge density of the impurity electrons.

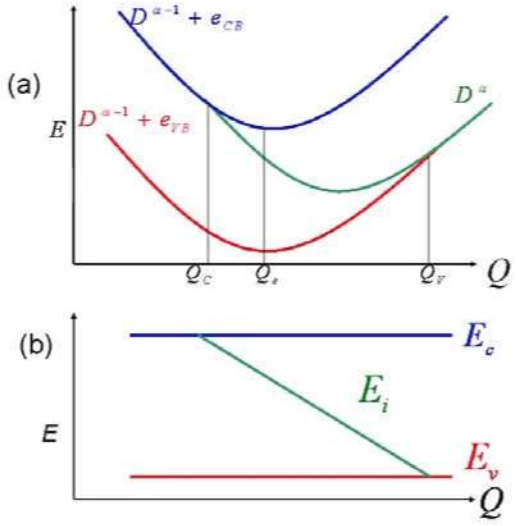

Figure 1: Schematic representation of the MPE-NRR recombination mechanism. (a) The curves represent the electronic energy of the $D^{\alpha-1}+e_{VB}$, D^{α}, and $D^{\alpha-1}+e_{CB}$ systems with respect to the configuration coordinate Q. e_{VB} and e_{CB} represent an electron in the VB and CB respectively. Q_V is the crossing point of the energy curves corresponding to the systems $D^{\alpha-1}+e_{VB}$ and D^{α}. Similarly, Q_C is the crossing point of the $D^{\alpha-1}+e_{CB}$ and D^{α} energy curves. (b) Impurity energy levels with respect to the VB and CB as a function of Q.

Formally, we know that the total electronic energy, in first approximation, is quadratic in Q near Q_0 when there is no impurity present (host solid without impurities):

$E = e_0 + K(Q-Q_0)^2/2$, where e_0 is the energy of the undistorted crystal and Q_0 is the equilibrium coordinate. The impurity in the state *i*, in first approximation, adds the extra term $e_i - G_i(Q-Q_0)$ to the total electronic energy, where e_i is the impurity energy when Q is the equilibrium coordinate Q_0, and G_i is the impurity force constant. Therefore, the total energy when the impurity+host is in the state *i* can be rewritten $E_i = E_i^{(0)} + K(Q-Q_i)^2/2$ where, $E_i^{(0)} = e_0 + e_i + E_R$, and $Q_i = Q_0 + G_i/K$. In this equation, $E_R = -G_i^2/2K$ is the impurity relaxation energy and G_i/K represents a shift in the equilibrium position of the host without impurity. Therefore, the displacement corresponding to two different states of the impurity in the host becomes $(Q_2 - Q_1) = (G_2 - G_1)/K$. Large displacements correspond to large forces variations (large changes in charge densities). While for deep gap levels these variations (ΔQ and ΔG) are large and the energy curves would cross, in the materials with an intermediate band analyzed there is a mechanism that regulates the charge density and impedes the NRR via MPE.

In order to diminish the NRR via MPE, it is found that when a charge is added to or eliminated from the IB due to electron capture processes it should be redistributed. In this case $\Delta G \approx \Delta Q \approx 0$ and in Fig.1 the minima of the energy curves will be located at about the same Q-value, and they would not cross.

There are two ways for which the crossing of the energy curves can be avoided: charge redistribution between all the impurities and charge redistribution with the host semiconductor. The former is related to the Mott transition [2]. In this work we analyze the latter mechanism. Anyway, there would be a small variation in the electronic density around the impurity atom.

In this study, we have chosen Cr-doped ZnS as material system. These materials have been analyzed previously both theoretically and experimentally. When Cr is used as dopant in ZnS this material shows experimentally [3] low non-radiative recombination and, as concluded from theoretical calculations [4], also an intermediate band (IB).

NRR is important in the half-filled IB materials. Solar cells based on these materials have an efficiency limit exceeding that of single gap solar cells [5]. Their properties are expected to be different from those of a material containing a group of deep energy levels because of this charge redistribution.

2 CALCULATIONS

All the calculations, based on the density-functional theory DFT [6] in the local-spin density approximation (LSDA), have been carried out using a supercell containing 64 atomic sites ($Cr_xZn_{1-x}S$ with x = 1/32). The standard Kohn–Sham (KS) [7] equations are solved self-consistently [8]. For the exchange and correlation term, the LSDA has been used as proposed by Ceperley–Alder [9]. The standard Troullier–Martins [10] pseudopotential is adopted and expressed in the Kleinman–Bylander [11] factorization. The KS orbitals are represented using a linear combination of confined pseudoatomic orbitals [12]. In all calculations, a double-zeta with polarization basis set has been used.

Several further corrections to the calculated energies [13] were applied: potential alignment between a charged defect calculation and the perfect host crystal, and spurious interaction of periodic image charges.

3 RESULTS

The electronic structure of isolated substitutional Cr in II-VI semiconductors is determined by the interaction between the 3*d*-orbitals of the impurity and the *p*-anion orbitals (p_A) of the VB. The calculations show an IB formed by spin-up states of *t* symmetry in the energy gap ($t_+^{(IB)} \approx c_1 \cdot d + c_2 \cdot p_A$) and a density of states of the same symmetry within the valence band ($t_+^{(VB)} \approx c_3 \cdot d + c_4 \cdot p_A$). This coexistence, in a similar energy range, of localized impurity states with delocalized host states with which charge can be exchanged is the key to the remarkable stability of various charge states. The chromium *3d* states can combine with the p_A states of the anions, thus providing an additional possibility of electronic density redistribution [14]. When the charge state of the Cr impurity and the configuration coordinates are changed by interaction with light (i.e., when an electron transits from the VB to the IB or from IB to CB), the excess charge (Δq) is redistributed through combination of the Cr-*d* states with the p_A states of the nearest neighbors, i.e. through the redistribution between the VB (Δq_{VB}) and IB (Δq_{IB}) in such a way that $\Delta q = \Delta q_{VB} + \Delta q_{IB} \approx 0$.

This behavior can be seen in Figure 2. In this figure, the modifications of the contribution of the *d*-Cr orbitals to the IB and to the VB as function of the configuration coordinate Q and of the IB charge q_{IB} are shown schematically. Because of this change, when the contribution of Cr to the IB increases, Δq_{IB} increases but Δq_{VB} decreases. Therefore, the charge density around of the impurity is almost constant ($\Delta q \approx 0$).

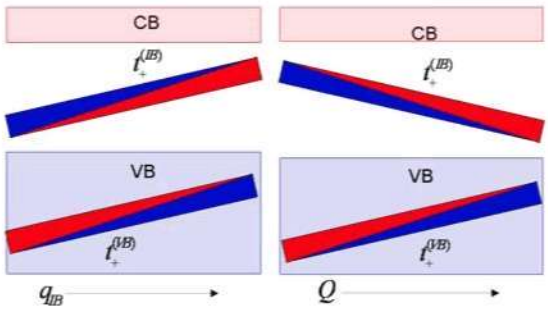

Figure 2: Schematic representation of the modification of the contributions of the impurity (red) and host (blue) to the antibonding $t_+^{(IB)}$ into the gap and to the bonding $t_+^{(VB)}$ into the VB as functions of the configuration coordinate Q and of the IB charge q_{IB}.

The electronic dynamics as a function of the atomic positions has been analyzed as well. We have considered the inward and outward displacement of the nearest neighbors of the Cr atom, i.e. breathing-modes, and the longitudinal modes, where the S atom in the (111) direction is displaced. The change in the contribution of the impurity atom to the IB and VB with the configuration coordinates of the breathing- and longitudinal-modes is shown schematically in Fig. 2. For the two modes, an inward relaxation increases the energy of the IB, and an outward relaxation diminishes it. An inward relaxation (reduction of Q) increases the overlap between the Cr-S orbitals, increasing the energy of the IB. Therefore, the IB has an antibonding character. Consequently, the outward movement (increase of Q) decreases the IB energy. Moreover, an inward (outward) movement decreases (increases) the Cr contribution to the IB.

Therefore, there is a self-regulation or Le Chatelier mechanism in response to adding charge to the IB and to the modifications of the equilibrium configuration through inward and outward movements of the breathing and longitudinal modes. The charge density around the impurity is equilibrated in response to these changes in charge and equilibrium configuration. This behavior is driven by the combination of two mechanisms: the interelectronic Coulomb repulsion and the modification of the bonding impurity-host.

According to the model previously described, $\Delta G \approx \Delta Q \approx 0$. Then, the minima of the energy curves will be at a similar Q, and the energy curves would not cross, except at very high energies. This can be seen in Fig. 3 where the energy curves obtained using first principles calculations corresponding to the steps $Cr^{+2}(d^4)+e_{VB} \rightarrow Cr^{+1}(d^5)$ and $Cr^{+1}(d^5) \rightarrow Cr^{+2}(d^4)+e_{CB}$ are shown for Cr-doped ZnS.

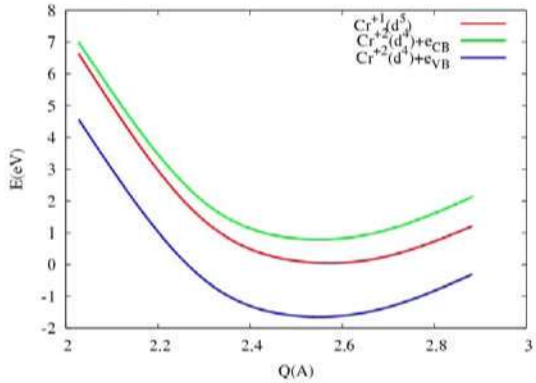

Figure 3: Configuration coordinate diagram in upward order of energy for $Cr^{+2}(d^4)+e_{VB}$, $Cr^{+1}(d^5)$ and $Cr^{+2}(d^4)+e_{CB}$ obtained from first-principles calculations.

Comparing the Figure 3 for Cr-doped ZnS, a material with an IB, with the Figure 1, typical of a deep impurity, it can be observed that in the former case there are no crossing points, except for high energies. This behavior has also been observed in Cr-doped ZnSe [12]. Our results show a lower relaxation energy: the difference between the equilibrium positions when the IB is modified varies by ±0.04 Å. The position of the minima of the energy curves is almost equal.

4 CONCLUSIONS

The behavior of a material with a partially filled intermediate band is very different from deep gap energy levels with respect to the NRR via MPE. The key difference arises from the variation of the electronic density around the impurities. While for deep gap levels these variations are larger, in the materials analyzed with an intermediate band, these variations are smaller and hinder NRR via MPE. When located within a proper host semiconductor, the IB favors the radiative transition rate over the non-radiative decay rate, an essential feature to approach the limiting efficiency predicted for these cells.

Among the materials analyzed, Cr-doped zinc chalcogenides, have shown promising properties. The results show that an increase in the impurity-host interactions leads to a decrease in both the difference between the equilibrium positions and the charge densities for different states. The delocalization of the electronic charge between the impurity and host is the fundamental mechanism to inhibit non-radiative recombination via MPE in these materials. It leads to small changes in the force constants between different states. This mechanism is additional to the one due to the increase of impurity concentration. In anycase a redistribution of the charge around of the impurities takes place.

This work represents one step forward in our understanding of the fundamentals that lead to the formation of a beneficial intermediate band with the desired recombination properties (inhibition of NRR) in contrast to conventional deep energy levels in semiconductors. This understanding allows to select, from ab-initio calculations, intermediate band material candidates that, not only show the required position of the intermediate band, but also the required recombination properties.

This work has been supported by the European Commission within the project IBPOWER (Contract 211640) and the projects NUMANCIA (S-0505/ENE/000310) funded by the Comunidad de Madrid and GENESISFV (CSD2006-0004) funded by the Spanish National Program.

REFERENCES

[1] C. H. Henry and D. V. Lang, *B* **15**, 989 (1977); D.V. Lang, C.H. Henry, *Phys.Rev.Lett.* **35,** 1525 (1975); K.V. Boer, *Survey of Semiconductor Physics*, John Wiley & Sons Inc (2002).
[2] A. Luque, A. Martí, E. Antolín and C. Tablero, *Physica B,* **382**, 320-327 (2006).
[3] L. D. DeLoach, R. H. Page, G. D. Wilke, S. A. Payne, and W. F. Krupke, *IEEE J. Quantum Electron.* **32**, 885 (1996); V.A. Kasiyan, R.Z. Shneck, Z.M. Dashevsky, S.R. Rotman, *Phys. Status Solidi* **229,** 395 (2002).
[4] C. Tablero, *Comp. Matter Sci.* **37**, 483 (2006); C. Tablero, *Sol. Energy Mat. Sol. C* **90**, 588 (2006); C. Tablero, *Phys. Rev. B. C* **74**, 195203 (2006).

[5] A. Luque and A. Martí, *Phys. Rev. Lett.* **78,** 5014 (1997).
[6] P. Hohenberg, W. Kohn, *Phys. Rev. B* **136** (1964) 864.
[7] W. Kohn, L.J. Sham, *Phys. Rev.* **140** (1965) A1133–A1138.
[8] J.M. Soler, E. Artacho, J.D. Gale, A. García, J. Junquera, P. Ordejon, D. Sánchez-Portal, *J. Phys. Condens. Matter* **14,** 2745 (2002) and references therein.
[9] D.M. Ceperley, B.J. Alder, *Phys. Rev. Lett.* **45** (1980) 566.
[10] N. Troullier, J.L. Martins, *Phys. Rev. B* **43** (1991) 1993.
[11] L. Kleinman, D.M. Bylander, *Phy. Rev. Lett.* **48** (1982) 1425; D.M. Bylander, L. Kleinman, Phys. Rev. B 41 (1990) 907.
[12] O.F. Sankey, D.J. Niklewski, *Phys. Rev. B* **40** (1989) 3979.
[13] C. Persson, Yu-Jun Zhao, S. Lany and A. Zunger, *Phys. Rev. B* **72**, 035211 (2005).
[14] C. Tablero, *Solid State Comun.* **143**, 399–402 (2007).